

A Novel Analysis of Delay and Power Consumption for Polling Schemes in the IoT

Li Feng, Jiguo Yu*, Feng Zhao, and Honglu Jiang

Abstract: In the Internet of Things (IoT), various battery-powered wireless devices are connected to collect and exchange data, and typical traffic is periodic and heterogeneous. Polling with power management is a very promising technique that can be used for communication among these devices in the IoT. In this paper, we propose a novel and scalable model to study the delay and the power consumption performance for polling schemes with power management under heterogeneous settings (particularly the heterogeneous sleeping interval). In our model, by introducing the concept of virtual polling interval, we successfully convert the considered energy-efficient polling scheme into an equivalent purely-limited vacation system. Thus, we can easily evaluate the mean and variance of the delay and the power consumption by applying existing queueing formulae, without developing a new theoretical model as required in previous works. Extensive simulations show that our analytical results are very accurate for both homogeneous and heterogeneous settings.

Key words: 802.11; Point Coordination Function (PCF); power management; queueing analysis

1 Introduction

The Internet of Things (IoT) has recently been defined as the infrastructure of the information society^[1]. In the IoT, various battery-powered wireless devices are connected to collect and exchange data. In such a network, typical flows are periodic and heterogeneous. For example, the environmental information (such as temperature) measured by sensors will be transmitted

periodically to computer-based systems; different flows may have different packet sizes and delay requirements. Conversely, different devices may have different power limits and sleeping intervals. When these heterogeneous devices coexist, delivering these periodic and heterogeneous flows in a timely and power-saving means is challenging.

There exist two types of typical wireless protocols for communication in the IoT, namely, contention-based and contention-free protocols. In contention-based protocols such as IEEE 802.11 Distributed Coordination Function (DCF), enhanced DCF channel access^[2], and variants of DCF^[3,4], each node must first contend for the channel and then transmit the packets. During the contention process, each node will continuously sense and listen to the channel constantly. When multiple nodes are simultaneously backing off, the entire channel remains idle. When multiple nodes transmit packets simultaneously, collisions occur. Thus the back-off and the collision will lead to serious channel under-utilization. It has been shown in Ref. [5] that more than 30% reduction in throughput is due to backing off. Conversely, it is difficult to guarantee a

• Li Feng is with Faculty of Information Technology, Macau University of Science and Technology, Macau, China. E-mail: lfeng@must.edu.mo.

• Jiguo Yu and Honglu Jiang are with School of Information Science and Engineering, Qufu Normal University, Rizhao 276826, China. E-mail: jiguoyu@sina.com; jianghonglu88@163.com.

• Feng Zhao is with School of Computer Science and Information Security, Guilin University of Electronic Technology, Guilin 541004, China. E-mail: zhaofeng@guet.edu.cn.

* To whom correspondence should be addressed.

Manuscript received: 2016-11-18; revised: 2016-12-31; accepted: 2017-01-18

timely packet delivery when the number of contending nodes is large and the traffic load is heavy. In addition, contention-based protocols are energy-consuming. In Ref. [6], it has been pointed out that idle listening is the dominant source of energy consumption in IEEE 802.11 networks and more than 60% of energy is consumed in idle listening, even with the power-saving mode enabled. Therefore, conventional 802.11 protocols are inapplicable to IoT. IEEE 802.15.4 is another type of contention-based protocol that is designed to communicate among battery-powered wireless sensors, and has attracted a great deal of attention^[7–11]. However, because of its randomness and distribution nature, it is not easy to guarantee the delay requirement while minimizing the power consumption for an 802.15.4 network.

In contrast, contention-free protocols such as the IEEE 802.11 Point Coordination Function (PCF)^[2], HCF Controlled Channel Access (HCCA)^[12], and the polling schemes in 802.11ah^[13] are potential candidates to satisfy the aforementioned IoT challenge. In contention-free protocols, for each period, each node is polled one-by-one for transmitting the packet, thereby eliminating contention and guaranteeing a timely packet delivery. When power-saving mode is enabled, the nodes will shift to sleep mode if no packets are transmitted or received and will keep receiving packets otherwise, thereby reducing the power consumption. However, despite substantial works^[14–18], there is still an absence of simple, accurate, and scalable models to study the performance of these schemes (in particular, using heterogeneous settings) to date. This motivates us to propose new performance models.

1.1 Our contributions

In this paper, we study the delay and power consumption of the PCF protocol with Power Management (PM), because it is the most fundamental polling scheme which has been extended to IEEE 802.11 HCCA^[12] and the latest 802.11ah protocol^[19]. Our contributions are summarized as follows:

- This paper first considers heterogeneous settings: heterogeneous traffic (i.e., heterogeneous frame arrival rate and frame size) and heterogeneous sleeping interval (i.e., different nodes have different sleeping periods).
- This paper proposes a novel simple, accurate, and scalable delay model. In our model, we successfully convert the PCF system with PM into an equivalent

purely-limited vacation system. Then, we apply the existing queueing formulae to easily evaluate the mean and variance of the delay without the need for developing a new model, as previously required in Ref. [16]. Our model is simple and applicable for heterogeneous settings and can evaluate the delay jitter performance of variance-sensitive applications such as voice over PCF. In contrast, Sikdar^[16] developed a theoretical model to study the mean delay using homogeneous settings; however, this model was tedious and complicated, and therefore is not easily extended to heterogeneous settings.

- This paper is the first to model the power consumption under heterogeneous settings.

Finally, we run extensive experiments to verify that the proposed model is very accurate.

1.2 Related work

In this paper, we develop a novel theoretical model to study the delay and the power consumption of the PCF with PM using heterogeneous settings. However, despite substantial existing works, most related works^[15–18] studied the performance of the PCF via simulation, instead of the PCF with PM. For example, Visser and Zarki^[17] investigated the throughput performance of the PCF via simulation. Wu and Huang^[18] presented a comparison study via simulation for four polling schemes including the PCF, while Granelli et al.^[14] investigated the power consumption of the PCF with PM via simulation.

There are a few theoretical studies on the performance of the PCF or the PCF with PM. Siddique and Kamruzzaman^[15] analyzed the MAC channel access delay of the PCF (which is the time interval between the frame reaching the head of the MAC queue and the frame being transmitted), but they did not analyze the total delay (including the channel access delay, frame transmission time, ACK time, and waiting delay). Sikdar^[16] developed an analytical framework to study the total delay for homogeneous settings in the PCF and the PCF with PM. This analytical framework had been extended to study the delay performance of wireless sensor networks^[20] and WiMAX^[21,22]. However, this analytical framework is tedious and complicated so extending it to heterogeneous settings appears to be difficult. Recently, our paper^[23] has proposed applying the classic exhaustive M/G/1 queueing model with multiple vacations to analyze the delay performance of the PCF, thereby avoiding

reconstructing a new analysis framework as performed in Ref. [16]. However, this paper did not study the delay with PM. Qiao et al.^[24] analyzed the energy-efficiency of the PCF that combines transmit power control with adaptive PHY rate selection. Palacios et al.^[25] roughly estimated the power consumption of the PCF. Both papers assumed homogeneous saturated traffic (where each node always has packets to transmit) and did not consider the feature of PM. In contrast, this paper studies the realistic heterogeneous unsaturated traffic and considers PM.

The rest of this paper is organized as follows. Section 2 provides an overview of the PCF protocol with PM. Section 3 proposes a delay model. Section 4 proposes a power consumption model. Section 5 validates our theoretical results via simulation, and Section 6 concludes this paper.

2 PCF with Power Management

In a wireless LAN, when the PCF and the DCF coexist, time is divided into a series of repetition intervals of equal length. In each repetition interval, the system runs first in the PCF mode and then in the DCF mode. In the PCF mode, there is a Point Coordinator (PC) and multiple stations.

The PCF defines a PM scheme to help stations conserve energy. In this scheme, a station alternates between two states: awake and doze states. In the awake state, a station is fully powered and may receive frames at any time. In the doze state, a station is unable to transmit or receive and consumes very low power. A station notifies the PC that its PM scheme is enabled and sets the sleeping interval parameter, i.e., the number of the repetition intervals for which the station is in the doze state. Then, the PC will buffer frames destined for the station when the station is in the doze state, and deliver one frame to the station for each repetition interval when the station is in the awake state.

The operational process of the PCF-PM scheme is explained in Fig. 1. After a PCF InterFrame Space (PIFS), the PC initializes a Contention-Free Period (CFP) by sending a beacon, marking the beginning of a new repetition interval. The Traffic Indication Map (TIM) field in the beacon contains a list of the stations whose frames have been buffered at the PC. When a station wakes up at the beginning of the repetition interval, it will listen to the TIM beacon. If it finds that its ID is not indicated in the TIM beacon, it will go to sleep mode immediately, as part of its sleeping interval. If it finds that its ID is indicated in the TIM beacon, it will keep awake until its polling opportunity, and then it begins receiving its buffered frame from the PC by following the pattern: SIFS/PS-Poll/SIFS/Data/SIFS/ACK.

Figure 1 illustrates that after stations 1 and 3 find themselves appearing in the list sequentially from the beacon, station 1 first waits for a Short InterFrame Space (SIFS), and then begins sending a polling frame [D1(PS-Poll)] to the PC. Once polled, the PC sends one data frame [D1(data)] to station 1 after a SIFS time. Receiving the data frame, station 1 sends back an acknowledgement (ACK) [D1(ACK)] to the PC. The process repeats until all stations in the list have polled the PC. Finally, the PC sends a CF-End control frame, marking the end of the current CFP. Hereafter, the system enters the DCF mode, in which the stations in the list can no longer receive data frames until the next repetition interval starts.

Remarks: The above PCF with PM is consistent with that in Ref. [16] but has two differences from that in Ref. [2]. First, for the downlink, this paper assumes the pattern: SIFS/PS-Poll/SIFS/Data/SIFS/ACK, but Ref. [2] defines the pattern: SIFS/Data/SIFS/ACK. Second, in this paper, we assume that if the AP has buffered packets to a station, the station remains awake; otherwise, the station enters the snooze state and then

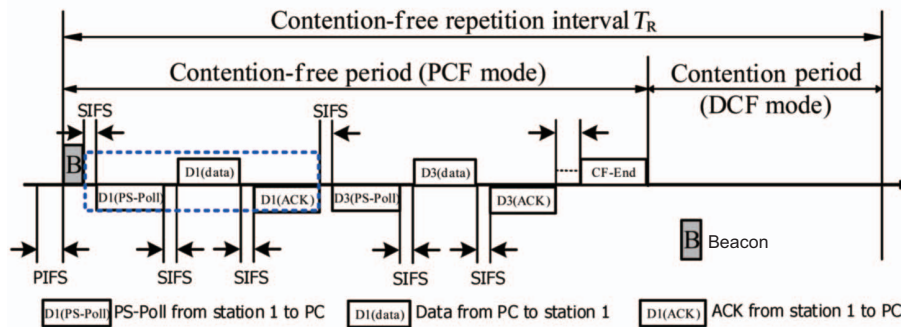


Fig. 1 PCF with PM.

wakes up for listening to the beacon after its sleeping interval. In contrast, in Ref. [2], the station listens to the beacon for every its sleeping interval. The first difference is trivial, as we retain this difference for a comparison with Ref. [16]. However, modeling the second difference accurately is not easy and is our ongoing research.

3 Proposed Delay Model

In this paper, focusing on the downlink traffic from the PC to the stations, we study the delay performance of the PCF with PM.

Let T_R denote the length of a repetition interval. For each station i ($1 \leq i \leq n$), we assume that the downlink traffic is a Poisson process with parameter λ_i , the data frame length is L_i , and the sleeping interval is $k_i T_R$, where k_i is a positive integer.

Let D_i denote the total delay of a tagged data frame of station i , where the total delay is defined to be the interval between when the tagged data frame arrives at the AP's MAC buffer and when the AP receives the ACK from the station i which receives the tagged frame. Let W_i denote the waiting time of the tagged packet of station i , where the waiting time is defined to be the interval between when the tagged data frame arrives at the AP's MAC buffer and when the AP starts to service station i . Let T_i denote the service time of the tagged data frame of station i , where the service time is defined to be the interval between when the AP starts to service station i (i.e., the instant after which station i first waits for a SIFS time and then sends a PS-Poll message to request its buffered frame from the AP) and when the AP receives the ACK from station i . Then, D_i is the sum of W_i and T_i , namely,

$$D_i = W_i + T_i, 1 \leq i \leq n \quad (1)$$

Note that the service process of a data frame follows the pattern: SIFS/PS-Poll/SIFS/Data/SIFS/ACK, as illustrated in Fig. 1. We can calculate T_i as follows:

$$T_i = 3T_{\text{SIFS}} + T_{\text{PS-Poll}} + T_{\text{frame},i} + T_{\text{ACK}} \quad (2)$$

where T_{SIFS} denotes the SIFS time, $T_{\text{PS-Poll}}$ denotes the PS-Poll time, $T_{\text{frame},i}$ denotes the transmission time of a data frame with length L_i , and T_{ACK} denotes the transmission time of the ACK frame.

Let $E(D_i)$ and $\text{Dev}\{D_i\}$ represent the mean and the standard deviation of the delay D_i , respectively. We have Eqs. (3) and (4).

$$E(D_i) = E\{W_i\} + T_i, 1 \leq i \leq n \quad (3)$$

$$\text{Dev}\{D_i\} = \text{Dev}\{W_i\} = \sqrt{E\{W_i^2\} - (E\{W_i\})^2} \quad (4)$$

The remaining task is to calculate $E\{W_i\}$ and $E\{W_i^2\}$. Below, we first outline the classic purely-limited vacation system, then convert the PCF-PM system into a pure limited vacation system, and finally derive the expressions of $E\{W_i\}$ and $E\{W_i^2\}$.

3.1 Classic purely-limited service system with multiple vacations

Here, we present the classic purely limited service system with multiple vacations^[26]. It is a single-server queueing system with an infinite buffer. In this system, customers arrive according to a Poisson process with rate λ , and the per-customer service time has a general distribution.

In this system, the server serves only one customer each time if any, and then takes a vacation immediately, no matter how many customers are waiting in the queue. Whenever the server returns from the ongoing vacation and finds no customers waiting in the queue, it will go on a new vacation; therefore, the server is said to take multiple vacations. According to the number of customers served before the server takes its vacations, we classify the vacations into two types: type 1 vacation with length V_1 (i.e., the vacation after a customer is served), and type 2 vacation with length V_2 (i.e., the vacation if no customer is served). Figure 2a illustrates that the server first takes two type 1 vacations

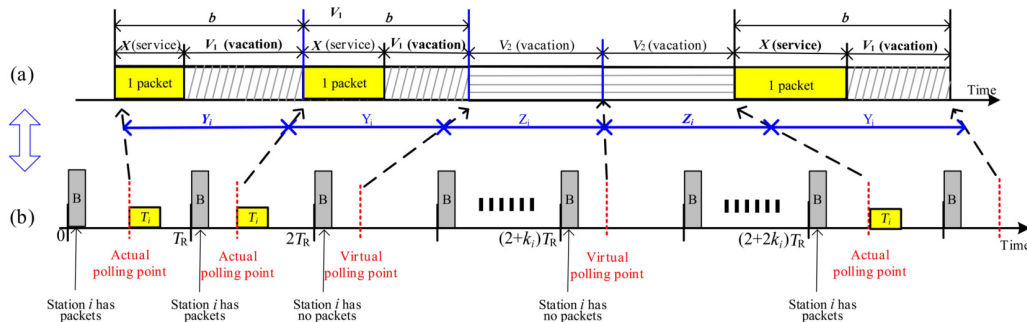


Fig. 2 (a) The classic purely-limited service system with multiple vacations, (b) the equivalent PCF-PM system.

sequentially, and then moves onto two type 2 vacations consecutively, before it begins serving a new customer.

Assume that the customers are served in the order they arrive. Let X be the service time of a customer, let $\beta = X + V_1$, and let W represent the waiting time of a customer before it is served. Let $W^*(s)$, $\beta^*(s)$, and $V_2^*(s)$ represent the Laplace transforms of the random variables W , β , and V_2 , respectively. From Section 2.6 in Ref. [26], $W^*(s)$ is given by

$$W^*(s) = \frac{1 - \lambda E\{\beta\}}{\lambda E\{V_2\}} \cdot \frac{V_2^*(s) - 1}{1 - \frac{s}{\lambda} - \beta^*(s)} \quad (5)$$

Note that $E\{W^n\} = (-1)^n (W^*(s))_{s=0}^{(n)}$, $E\{\beta^n\} = (-1)^n (\beta^*(s))_{s=0}^{(n)}$, and $E\{V_2^n\} = (-1)^n (V_2^*(s))_{s=0}^{(n)}$ by the basic property of Laplace transform. We can calculate $E\{W\}$ and $E\{W^2\}$ as follows:

$$E\{W\} = f_1(\lambda, \rho, \beta, V_2) \triangleq \frac{\lambda E\{\beta^2\}}{2(1 - \rho)} + \frac{E\{V_2^2\}}{2E\{V_2\}} \quad (6)$$

and

$$E\{W^2\} = f_2(\lambda, \rho, \beta, V_2) \triangleq \frac{\lambda E\{\beta^3\}}{3(1 - \rho)} + \frac{[\lambda E\{\beta^2\}]^2}{2(1 - \rho)^2} + \frac{\lambda E\{\beta^2\} E\{V_2^2\}}{2(1 - \rho)E\{V_2\}} + \frac{E\{V_2^3\}}{3E\{V_2\}} \quad (7)$$

where $E\{\cdot\}$ denotes the mean of “ \cdot ” and the traffic intensity $\rho = \lambda E\{\beta\}$.

3.2 Equivalent purely-limited vacation system

Now, we first convert the PCF-PM system into an equivalent purely limited vacation system, and then express $E\{W_i\}$ and $E\{W_i^2\}$ of the PCF-PM system.

We start describing the equivalent relationship from the receiving process that the station receives a frame from the AP. Consider a station i in the PCF-PM system. Consider station i as a server. Regard the frames (arriving from the AP to station i) as the customers of the server, where frame arrivals follow a Poisson process with parameter λ_i . When station i wakes up, it will receive a frame if it determines that its TIM beacon contains its ID, otherwise it will continue to snooze. Equivalently speaking, station i will actually serve a customer for a duration of T_i if it determines that its TIM beacon contains its ID, or it will virtually serve a customer for a duration of 0 s (i.e., station i will not serve a customer) otherwise.

Define the actual (virtual) polling point of a station i , to be the instant that station i begins serving an actual or virtual frame, namely the instant after the previous ($i - 1$)-th station actually or virtually serves frames. The actual (virtual) polling points are illustrated in Fig. 2b.

Let Y_i represent the actual polling interval between an actual polling point of station i and its next actual or virtual polling point. According to the PCF-PM system, a station will receive only one frame in the interval Y_i .

Let Z_i represent the virtual polling interval between a virtual polling point of station i and its next actual or virtual polling point. According to the PCF-PM system, a station will not receive any frame in the interval, Z_i .

Therefore, in an actual or virtual polling interval, station i will receive at most one frame and then it either remains idle or goes to sleep; that is, station i goes on vacation when it either remains idle or goes to sleep, because it will not receive any frame during that time.

Equivalent purely-limited rules: The instruction in the PCF-PM system that a station will receive at most one frame in an actual or virtual polling interval, is naturally consistent with the purely-limited rule that the server serves only one customer each time, if any.

Equivalent vacation rules: The time in the PCF-PM system that a station either remains idle or goes to sleep in an actual or virtual polling interval, is naturally regarded as the vacation time in the purely-limited vacation system, where the server will not serve any customer once it takes a vacation, no matter how many customers are waiting in the queue. The fact that a station in the PCF-PM system will take another vacation if it wakes up and does not find its identify in the received beacon, is naturally consistent with the concept of multiple vacations in the purely-limited vacation system. In addition, the actual polling interval Y_i in the PCF-PM system (in which station i first serves a frame and then remains idle) is equivalent to the interval β in the purely-limited vacation system; the virtual polling interval Z_i in PCF-PM (in which station i goes to sleep) is equivalent to the interval V_2 in the purely-limited vacation system.

In short, from the viewpoint of station i , the PCF-PM system can be regarded as an equivalent purely-limited vacation system, where

$$\beta = Y_i, V_2 = Z_i \quad (8)$$

Then, from Eqs. (6)–(8), we can easily calculate

$$E\{W_i\} = f_1(\lambda_i, \rho_i, Y_i, Z_i),$$

$$E\{W_i^2\} = f_2(\lambda_i, \rho_i, Y_i, Z_i) \quad (9)$$

where the traffic intensity $\rho_i = \lambda_i E\{Y_i\}$.

To evaluate $E\{W_i\}$ and $E\{W_i^2\}$ in Eq. (9), in the next two subsections, we calculate the n -th moment of Y_i and Z_i , respectively, where $n = 1, 2, 3$.

3.3 Calculation of $E\{Y_i\}$, $E\{Y_i^2\}$, and $E\{Y_i^3\}$

We first express Y_i with the help of Fig. 3. According to the definition of Y_i , we have

$$Y_i = T_R + \eta_i^{(2)} - \eta_i^{(1)} \quad (10)$$

where T_R denotes the length of a repetition interval, $\eta_i^{(1)}$ denotes the actual polling point of station i in the first repetition interval, and $\eta_i^{(2)}$ denotes the actual or virtual polling point of station i in the second repetition interval.

In our model, $\eta_i^{(1)}$ and $\eta_i^{(2)}$ are independent and identically distributed (i.i.d.) with a generic random variable η_i . We explained the reason as follows. As illustrated in the first repetition interval in Fig. 3, station i begins its service only if station j , $1 \leq j \leq i-1$, has completed its service. Therefore, we express η_i as follows:

$$\eta_i = T_B + \sum_{j=1}^{i-1} \xi_j \quad (11)$$

where T_B is the beacon transmission time and ξ_j ($1 \leq j \leq i-1$) is a random variable denoting the service time of station j . The duration of ξ_j depends on whether station j is in the awake or snooze state. Note that in each repetition interval of T_R , station j is in the awake state with probability $\rho_j = \lambda_j E\{Y_j\} = \lambda_j T_R$ (because it has packets with probability ρ_j) and it is in the snooze state with probability $1 - \rho_j$. ξ_j is equal to T_j with probability ρ_j , and 0 with probability $1 - \rho_j$. We can write ξ_j as follows:

$$\xi_j = \begin{cases} T_j, & \text{w.p. } \rho_j; \\ 0, & \text{w.p. } 1 - \rho_j \end{cases} \quad (12)$$

In Eq. (12), we essentially assume that ξ_j in one repetition interval is i.i.d. with that in another repetition interval. In addition, note that: (1) in each repetition interval, ξ_i is independent of ξ_j for $i \neq j$ since the frame arrival at each station is independent, and (2) the functions of independent random variables are also independent. We conclude that $\eta_i^{(1)}$ and $\eta_i^{(2)}$ are i.i.d. with η_i .

We next calculate the variance of η_i , $\text{Var}\{\eta_i\}$. From Eq. (12), we have

$$E\{\xi_j\} = T_j \rho_j, \quad E\{\xi_j^2\} = T_j^2 \rho_j,$$

$$\text{Var}\{\xi_j\} = E\{(\xi_j)^2\} - (E\{\xi_j\})^2 = (T_j^2 - T_j) \rho_j \quad (13)$$

Since all ξ_j s are independent each other, from Eqs. (11) and (13), we have

$$\text{Var}\{\eta_i\} = \sum_{j=1}^{i-1} \text{Var}\{\xi_j\} = \sum_{j=1}^{i-1} (T_j^2 - T_j) \rho_j \quad (14)$$

We finally calculate the n -th moment of Y_i , where $n = 1, 2, 3$.

$$E\{Y_i\} = E\{T_R + \eta_i^{(2)} - \eta_i^{(1)}\} = T_R \quad (15)$$

and

$$\begin{aligned} E\{Y_i^2\} &= E\{(T_R + \eta_i^{(2)} - \eta_i^{(1)})^2\} = \\ &= T_R^2 + E\{(\eta_i^{(2)} - \eta_i^{(1)})^2\} = \\ &= T_R^2 + 2(E\{\eta_i^2\} - (E\{\eta_i\})^2) = \\ &= T_R^2 + 2\text{Var}\{\eta_i\} = \\ &= T_R^2 + 2 \sum_{j=1}^{i-1} (T_j^2 - T_j) \rho_j \end{aligned} \quad (16)$$

$$\begin{aligned} E\{Y_i^3\} &= E\{(T_R + \eta_i^{(2)} - \eta_i^{(1)})^3\} = \\ &= E\{T_R^3\} + 3T_R E\{(\eta_i^{(2)} - \eta_i^{(1)})^2\} + E\{(\eta_i^{(2)} - \eta_i^{(1)})^3\} = \\ &= T_R^3 + 6T_R \text{Var}\{\eta_i\} + E\{(\eta_i)^3\} - 3E\{(\eta_i)^2\} \times \\ &= E\{\eta_i\} + 3E\{\eta_i\} E\{(\eta_i)^2\} - E\{(\eta_i)^3\} = \\ &= T_R^3 + 6T_R \text{Var}\{\eta_i\} = T_R^3 + 6T_R \sum_{j=1}^{i-1} (T_j^2 - T_j) \rho_j \end{aligned} \quad (17)$$

where we use $E\{(\eta_i^{(2)} - \eta_i^{(1)})^3\} = 0$ in Eq. (17).

3.4 Calculation of $E\{Z_i\}$, $E\{Z_i^2\}$, and $E\{Z_i^3\}$

Here, we first express Z_i , with the help of Fig. 4. According to the definition of Z_i , we have

$$Z_i = k_i T_R + \eta_i^{(2)} - \eta_i^{(1)} \quad (18)$$

where $k_i T_R$ is the sleeping interval length of station i , $\eta_i^{(1)}$ and $\eta_i^{(2)}$ are defined in Eq. (10) and are i.i.d. with η_i in Eq. (11).

We then calculate the n -th moment of Z_i , where $n = 1, 2, 3$, following the derivation process in Section 3.3.

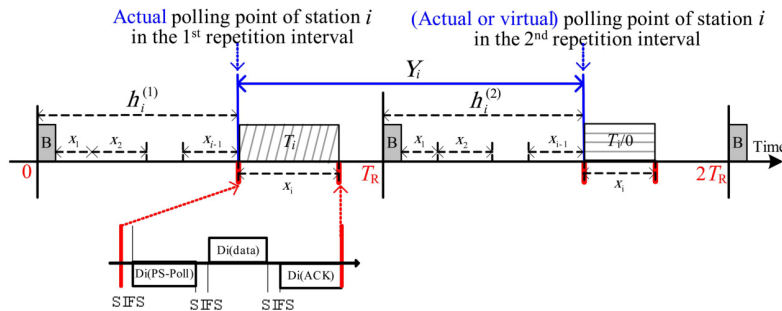


Fig. 3 Actual polling interval.

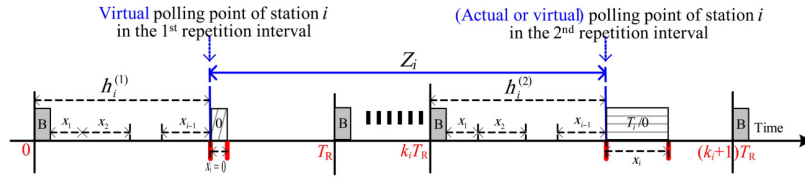


Fig. 4 Virtual polling interval.

$$\begin{aligned}
 E\{Z_i\} &= k_j T_R, \\
 E\{Z_i^2\} &= (k_j T_R)^2 + 2 \sum_{j=1}^{i-1} (T_j^2 - T_j) \rho_j, \\
 E\{Z_i^3\} &= (k_j T_R)^3 + 6(k_j T_R) \sum_{j=1}^{i-1} (T_j^2 - T_j) \rho_j
 \end{aligned} \tag{19}$$

4 Proposed Power Consumption Model

In this section, we study the power consumption of the PCF system with PM, namely, PCF-PM.

For the PCF-PM system, a station alternates between two states: snooze and awake states. In the snooze state, the station goes to sleep and consumes very low power; in the paper, we assume that the power consumption in the snooze state is zero. In the awake state, the power consumption can be classified into two types:

- power consumption P_{rx} when the station is in the reception mode.
- power consumption P_{tx} when the station is in the transmission mode.

Let $PW_{i,1}$ denote the power consumption of station i during a time interval of T_R where it is in the awake state. In the time interval of T_R , the station is in the transmission mode only when it transmits an ACK frame and a PS-Poll frame, and is in the reception mode for all other times. We have

$$PW_{i,1} = ((T_R - T_{ACK} - T_{PS-Poll})P_{rx} + (T_{ACK} + T_{PS-Poll})P_{tx}) / T_R.$$

Let $PW_{i,2}$ denote the power consumption of station i during a time interval of $k_i T_R$. In the time interval of $k_i T_R$, the station continues to receive a beacon for a time of T_B at the beginning of this interval, and finds no packet arrivals and therefore enters the snooze state. We have

$$PW_{i,2} = \frac{T_B P_{rx}}{k_i T_R}.$$

Let Φ_i denote the power consumption of station i . Note that station i enters the awake state with probability ρ_i and consumes power of $PW_{i,1}$, or enters the snooze state with probability $1 - \rho_i$ and consumes power of $PW_{i,2}$. We have

$$\Phi_i = \begin{cases} PW_{i,1}, & \text{w.p. } \rho_i; \\ PW_{i,2}, & \text{w.p. } 1 - \rho_i. \end{cases}$$

Let $E(\Phi_i)$ and $\text{Dev}\{\Phi_i\}$ represent the mean and the standard deviation of the power consumption Φ_i , respectively. Then, we have

$$E(\Phi_i) = \rho_i PW_{i,1} + (1 - \rho_i) PW_{i,2} \tag{20}$$

$$\text{Dev}\{\Phi_i\} = \text{Dev}\{\Phi_i\} = \sqrt{E\{\Phi_i^2\} - (E\{\Phi_i\})^2} \tag{21}$$

5 Model Verification

In this section, we verify our delay and power consumption model of the PCF-PM system under heterogeneous settings (i.e., heterogeneous frame arrival rate, frame size, and sleeping interval). In our simulation, the default parameter values, in accordance with 802.11b, are shown in Table 1, where 1 slot = $T_{\text{slot}} = 20 \mu\text{s}$, and time is measured in slots, the IP routing header = 20 bytes, the length of the Frame Check Sequence (FCS) = 4 bytes, and the number of stations $n = 8$. The buffer size for each station and the PC is set to 1000 data frames. Each simulation value is

Table 1 Default parameter settings that are used in this paper.

Parameter	Value
PHYHeader	24 bytes
MACHeader	32 bytes
RouteHeader	20 bytes
FCS	4 bytes
T_{slot}	20 μs
T_{SIFS}	10 μs
T_R	15 ms
n	8
R_{data}	11 Mbps
R_{basic}	1 Mbps
$T_{\text{PS-Poll}}$	$(\text{PHYHeader} + \text{MACHeader} + \text{FCS}) / R_{\text{basic}}$
T_{header}	$\text{PHYHeader} / R_{\text{basic}} + (\text{MACHeader} + \text{FCS}) / R_{\text{data}}$
T_{ACK}	T_{header}
T_B	209 μs
$T_{\text{frame},i}$	$T_{\text{header}} + (\text{RouteHeader} + L_i) / R_{\text{data}}$
P_{tx}	900 mW
P_{rx}	550 mW

an average over four simulation runs, where each run is 400 s.

We assume Poisson arrivals and run two experiments. In the first experiment, we consider the homogeneous settings, where all stations have the same data frame arrival rate, the same data frame size of 100 bytes, and the same sleeping interval of $5T_R$. In the second experiment, we consider the heterogeneous settings, where stations 1 to 4 transmit voice traffic^[27] and stations 5 to 8 transmit data traffic at a rate of 11 Mbps (i.e., $R_{\text{data}} = 11$ Mbps), and each station takes a different parameter setting, as shown in Table 2. For each experiment, we simulate the total delay and the power consumption, and verify the accuracy of our theoretical models by comparing the theoretical and simulation results.

5.1 Total delay

The mean total delay of station 8's data frames as a function of the data frame arrival rate for homogeneous settings (note that we obtain very similar results when considering other station's data frame) is illustrated in Fig. 5. The dashed curve shows the simulation

Table 2 Parameter values for voice traffic^[27] and data traffic.

	Station ID	λ_i (packets/s)	L_i (bytes)	$k_i (T_R)$
Voice traffic	1	16.67	48	2
	2	25.00	40	3
	3	33.33	50	4
	4	50.00	160	5
Data traffic	5	20.00	500	6
	6	30.00	600	7
	7	40.00	700	8
	8	50.00	800	9

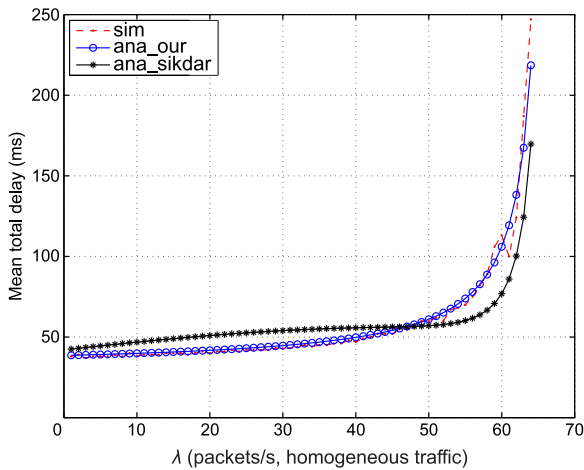


Fig. 5 Mean total delay as a function of data frame arrival rate for the homogeneous settings.

results, while the solid curve labeled with “ana_our” represents our theoretical result and the solid curve labeled with “ana_sikdar” represents the theoretical result in Ref. [16], which is calculated by the setting in this paper. From Fig. 5, we can see that our results better match the corresponding simulation results than those in Ref. [16], indicating that our delay model is more accurate.

Figure 6a displays the mean total delay (Eq. (3)) and Fig. 6b displays the standard deviation (Eq. (4)) of the total delay, where the abscissa represents the station ID. The bar with the dashed border represents the simulation results, while the bar with the solid border represents the theoretical results. Note that the standard deviation of the total delay is identical to that of the waiting delay since T_i in Eq. (1) is constant. From Fig. 6, each station has apparently different delay mean and variance since each station takes a very different parameter setting. The close match between

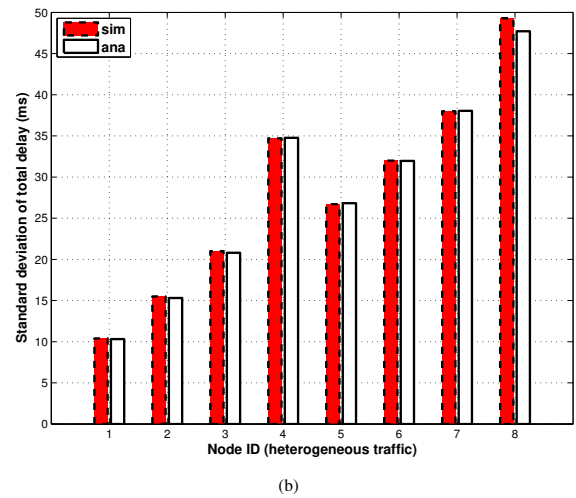
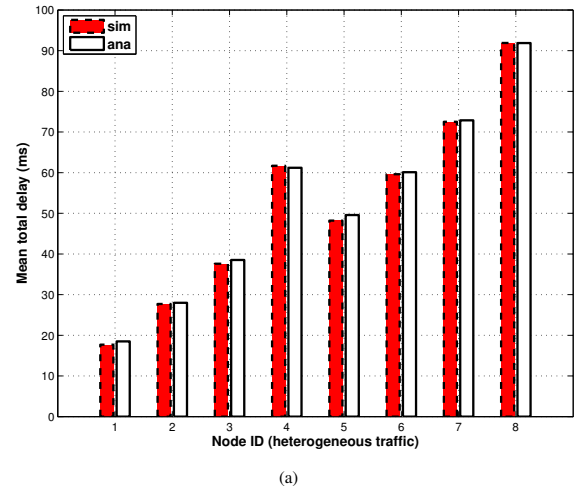


Fig. 6 (a) Mean and (b) standard deviation of total delay as a function of station ID for the heterogeneous settings.

the theoretical curves and the corresponding simulation curves manifests that our delay model is also very accurate for heterogeneous settings.

5.2 Power consumption

The mean power consumption of station 8’s data frames as a function of the data frame arrival rate for the homogeneous settings (note that we obtain very similar results when considering other station’s data frame) is illustrated in Fig. 7. The dashed curve shows the simulation results, while the solid curve labeled with “ana_our” represents our theoretical result, based on Eq. (20). From Fig. 7, one observes that as the frame arrival rate increases, the power consumption increases linearly. This is because the mean power consumption shown in Eq. (20) is a linear function of the frame arrival rate λ . The close match between the theoretical curves and the corresponding simulation curves manifests that our energy model is very accurate using the homogeneous settings.

Figure 8a plots the mean power consumption and Fig. 8b plots the standard deviation of the power consumption, where the abscissa represents the station ID. The bar with the dashed border represents the simulation results, while the bar with the solid border represents the theoretical results. From Fig. 8, for each station, the mean power consumption is apparently different, but the standard deviation of the power consumption is typically a fixed value (i.e., 250 mW in this example). This is a result of the combined effects due to the settings of the traffic parameters, such as frame arrival rate, power parameters, and sleeping interval. The close match between the theoretical curves

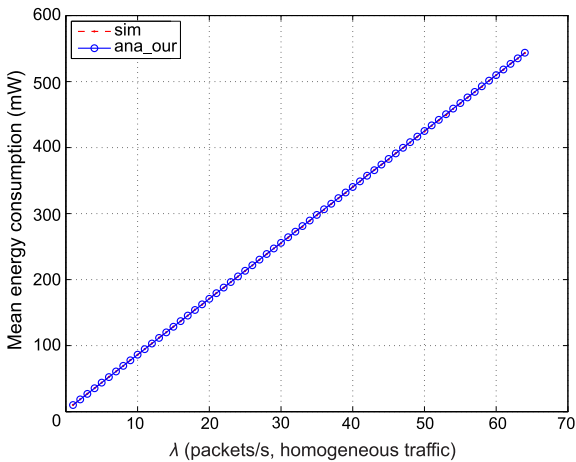
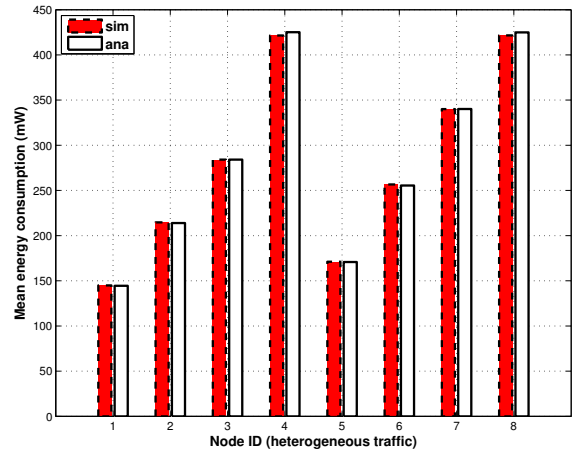
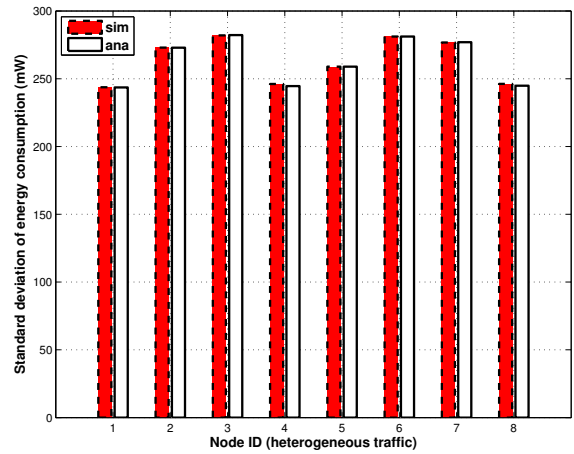


Fig. 7 Mean energy consumption as a function of data frame arrival rate for the homogeneous settings.



(a)



(b)

Fig. 8 (a) Mean and (b) standard deviation of energy consumption as a function of station ID for the heterogeneous settings.

and the corresponding simulation curves manifests that our energy model is also very accurate for heterogeneous settings.

6 Conclusion

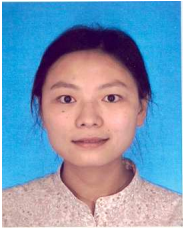
This paper studies the delay and power consumption performance of polling schemes with PM for the IoT. In the IoT, the traffic is diverse and heterogeneous, while wireless devices are often battery-powered and have different sleeping intervals. Therefore, our main goal was to investigate the impact of heterogeneous traffic and heterogeneous sleeping intervals on the system performance. Compared with related works, our model is simpler, more accurate, and more applicable for both homogeneous and heterogeneous settings. Extensive simulations verify that our model is very accurate.

Acknowledgment

This work was supported by Macao FDCT-MOST grant 001/2015/AMJ, Macao FDCT grants 013/2014/A1 and 005/2016/A1, the National Natural Science Foundation of China (Nos. 61373027 and 61672321), and the Natural Science Foundation of Shandong Province (No. ZR2012FM023).

References

- [1] IoTGSI, Internet of things global standards initiative, 2006. Available: <http://www.itu.int/en/ITU-T/gsi/iot/Pages/default.aspx>, Accessed on July 6, 2015.
- [2] ANSI/IEEE Std 802.11, Part 11: Wireless LAN Medium Access Control (MAC) and Physical Layer (PHY) Specifications, 1999 Edition (R2003), 1999.
- [3] L. Feng, J. Yu, X. Cheng, and M. Atiquzzaman, A novel contention-on-demand design for WiFi hotspots, *Personal and Ubiquitous Computing*, vol. 20, no. 5, pp. 705–716, 2016.
- [4] L. Feng, J. Yu, X. Cheng, and S. Wang, Analysis and optimization of delayed channel access for wireless cyber-physical systems, *EURASIP J. Wireless Comm. and Networking*, vol. 60, pp. 1–13, 2016.
- [5] A. Jardosh, K. Ramachandran, K. Almeroth, and E. Belding-Royer, Understanding congestion in IEEE 802.11b wireless networks, in *Internet Measurement Conference 2005*, 2005, pp. 279–292.
- [6] X. Zhang and K. Shin, E-MiLi: Energy-minimizing idle listening in wireless networks, *IEEE Transactions on Mobile Computing*, vol. 11, no. 9, pp. 1441–1454, 2012.
- [7] J. Yu, N. Wang, and G. Wang, Constructing minimum extended weakly-connected dominating sets for clustering in ad hoc networks, *Journal of Parallel Distributed Computing*, vol. 72, no. 1, pp. 35–47, 2012.
- [8] J. Yu, Y. Qi, G. Wang, Q. Guo, and X. Gu, An energy-aware distributed unequal clustering protocol for wireless sensor networks, *International Journal of Distributed Sensor Networks*, vol. 2011, no. 5, pp. 876–879, 2011.
- [9] J. Yu, L. Feng, L. Jia, X. Gu, and D. Yu, A local energy consumption prediction-based clustering protocol for wireless sensor networks, *Sensors*, vol. 14, no. 12, pp. 23017–23040, 2014.
- [10] G. Wang, J. Yu, D. Yu, H. Yu, L. Feng, and P. Liu, DS-MAC: An energy efficient demand sleep MAC protocol with low latency for wireless sensor networks, *Journal of Network and Computer Applications*, vol. 58, pp. 155–164, 2015.
- [11] X. Gu, J. Yu, D. Yu, G. Wang, and Y. LV, ECDC: An energy and coverage-aware distributed clustering protocol for wireless sensor networks, *Computers & Electrical Engineering*, vol. 40, no. 2, pp. 384–398, 2014.
- [12] IEEE Std 802.11e, Specific requirements Part 11: Wireless LAN Medium Access Control (MAC) and Physical Layer (PHY) Specifications, Amendment 8: Medium Access Control (MAC) Quality of Service Enhancements, 2005.
- [13] T. Adame, A. Bel, B. Bellalta, J. Barcelo, and M. Oliver, IEEE 802.11ah: The WiFi approach for m2m communications, *IEEE Wireless Commun.*, vol. 21, no. 6, pp. 144–152, 2014.
- [14] F. Granelli, R. Palacios, D. Gajic, C. Lis, and D. Kliazovich, An energy-efficient point coordination function using bidirectional transmissions of fixed duration for infrastructure IEEE 802.11 WLANs, in *Proc. IEEE ICC 2013*, 2013, pp. 2443–2448.
- [15] M. A. R. Siddique and J. Kamruzzaman, Performance analysis of PCF based WLANs with imperfect channel and failure retries, in *Proc. IEEE GLOBECOM 2010*, 2010, pp. 1–6.
- [16] B. Sikdar, An analytic model for the delay in IEEE 802.11 PCF MAC-based wireless networks, *IEEE Trans. Wireless Commun.*, vol. 6, no. 4, pp. 1542–1550, 2007.
- [17] M. Visser and M. Zarki, Voice and data transmission over an 802.11 wireless network, in *Proc. IEEE PIMRC 1995*, 1995, pp. 648–652.
- [18] J. Wu and G. Huang, Simulation study based on QoS schemes for IEEE 802.11, in *Proc. 3rd International Conference on Advanced Computer Theory and Engineering (ICACTE)*, 2010, pp. 534–538.
- [19] IEEE 802.11ah Task Group, 11/1137r14 Specification Framework for TGah, 2006. Available: http://www.ieee802.org/11/Reports/tgah_update.htm, Accessed on January 7, 2016.
- [20] H. Yang and B. Sikdar, Queueing analysis of polling based wireless MAC protocols with sleep-wake cycles, *IEEE Trans. Commun.*, vol. 60, no. 9, pp. 2427–2433, 2012.
- [21] R. Iyengar and B. Sikdar, A queueing model for polled service in WiMAX/IEEE 802.16 Networks, *IEEE Trans. Commun.*, vol. 60, no. 7, pp. 1777–1781, 2012.
- [22] B. Sikdar, Queueing analysis of polled service classes in the IEEE 802.16 MAC protocol, *IEEE Trans. Wireless Commun.*, vol. 8, no. 12, pp. 5767–5772, 2009.
- [23] L. Feng, J. Li, and X. Lin, A new delay analysis for IEEE 802.11 PCF, *IEEE Transactions on Vehicular Technology*, vol. 62, no. 8, pp. 4064–4069, 2013.
- [24] D. Qiao, S. Choi, A. Soomro, and K. Shin, Energy-efficient PCF operation of IEEE 802.11a wireless LAN, in *Proc. IEEE INFOCOM 2002*, 2002, pp. 580–589.
- [25] R. Palacios, G. Mekonnen, J. Alonso-Zarate, D. Kliazovich, and F. Granelli, Analysis of an energy-efficient MAC protocol based on polling for IEEE 802.11 WLANs, in *Proc. IEEE ICC 2015*, 2015, pp. 5941–5947.
- [26] H. Takagi, *Queueing Analysis*, Volume 1. North-Holland Amsterdam, 1991.
- [27] Q. L. Zhao, D. H. K. Tsang, and T. Sakurai, A simple critical-offered-load-based CAC scheme for IEEE 802.11 DCF networks, *IEEE/ACM Transactions on Networking*, vol. 19, no. 5, pp. 1485–1498, 2011.



Li Feng received the MS degree from the University of Hong Kong, China in 2007, and the PhD degree from Macau University of Science and Technology (MUST), China in 2013. Now she is an assistant professor in FIT, MUST. Her research interests include wireless and mobile networks, power saving, SDN, and network performance analysis.



Jiguo Yu received the PhD degree from Shandong University in 2004. He became a full professor with the School of Computer Science, Qufu Normal University, China, in 2007. He is currently a full professor with the School of Information Science and Engineering, Qufu Normal University. His main research interests include wireless networking, distributed algorithms, privacy-aware computing, peer-to-peer computing, and graph theory. He is interested in designing and analyzing algorithms for computationally hard problems in networks. He is a member of ACM and a senior member of the China Computer Federation.



Feng Zhao received the PhD degree in communication and information system from Shandong University, China, in 2007. He is currently a professor with the School of Information and Communications, Guilin University of Electronic Technology. His research interests include cognitive radio networks, MIMO wireless communications, cooperative communications, and smart antenna techniques.



Honglu Jiang received the BS and MS degrees in computer science from Qufu Normal University in 2009 and 2012, respectively. She is currently a PhD candidate in School of Information Science and Engineering at Qufu Normal University. Her research interests include wireless networks, distributed computing, and privacy preserving.